

Modelling bond between corroded reinforcement and concrete

K.Lundgren

Department of Structural Engineering, Chalmers University of Technology, Gothenburg, Sweden

ABSTRACT: The bond mechanism between deformed bars and concrete is known to be influenced by a number of parameters, such as the strength of the surrounding structure, yielding of the reinforcement, and corrosion of the reinforcement. A new model of the bond mechanism was developed, where the splitting stresses of the bond action are included, and the bond stress depends not only on the slip, but also on the radial deformation between the reinforcement bar and the concrete. The volume increase due to corrosion of the reinforcement is modelled, together with the mechanical behaviour of the corrosive products. Finite element analyses of corrosion cracking tests, and pull-out tests with corroded and uncorroded reinforcement were carried out. Reasonably good agreement between test results and analyses was obtained. Cracking appeared at about the same corrosion level as in experiments, and the decrease of bond due to splitting of the concrete could be predicted.

1 INTRODUCTION

The bond between deformed bars and concrete is known to be influenced by for example splitting cracks and yielding of the reinforcement. A new model was developed, which is specially suited for detailed three-dimensional analyses. In this new model, the splitting stresses of the bond action are included, and the bond stress depends not only on the slip, but also on the radial deformation between the reinforcement bar and the concrete. Thereby, the influence of the surrounding structure is included, so that the bond stress will decrease if the concrete split, or the reinforcement starts yielding.

Corrosion of the reinforcement often determines the durability of concrete structures. Since corrosion of reinforcement causes a volume increase, splitting stresses are induced in the concrete. Thus, there is a strong interaction between corrosion of the reinforcement and the bond mechanism.

The bond model is here combined with the modelling of a corrosion layer. With this way of modelling, one set of input parameters is given for the interface between the steel and the concrete. Depending on the applied corrosion level, and on the confinement of the modelled surrounding structure, various bond-slip curves result. The modelling of the combined corrosion and bond layer is presented here, together with results from finite element analyses of pull-out tests and corrosion cracking tests.

2 INTERFACE ELEMENTS

The modelling method described in this paper is specially suited for detailed three-dimensional finite element analyses, where both the concrete and the reinforcement are modelled with solid elements. The finite element program DIANA was used. There, interface elements are available which describe a relation between the traction \mathbf{t} and the relative displacement \mathbf{u} in the interface. These interface elements are used at the surface between the reinforcement bars and the concrete. The variables t_n , t_t , u_n and u_t are used for describing the stresses and deformation in the interface layer. The physical interpretation of t_t is the bond stress, t_n stands for the normal splitting stress, u_t is the slip, and u_n is the relative normal deformation between the reinforcement and the concrete. The corrosion model and the bond model can be viewed as two separate layers around a reinforcement bar. Due to equilibrium between the two layers, the traction \mathbf{t} is the same in the bond and in the corrosion layer. The deformations are related as:

$$u_n = u_{ncor} + u_{nbond} \quad (1)$$

$$u_t = u_{tbond}, \quad u_{tcor} = 0 \quad (2)$$

where the index *cor* means for the corrosion layer, and the index *bond* means for the bond layer. Equa-

tions (1) and (2) are solved within the interface element, together with the condition for equilibrium. For more information about the implementation, see Lundgren (2000b).

3 BOND MODEL

3.1 Presentation of the bond model

The model of the bond mechanism is presented in greater detail by Lundgren & Gylltoft (2000), and by Lundgren (1999). Here, a brief summary of the model is given. The bond model is a frictional model, using elasto-plastic theory to describe the relations between the stresses and the deformations. The relation between the tractions \mathbf{t} and the relative displacements \mathbf{u} is in the elastic range:

$$\begin{bmatrix} t_n \\ t_t \end{bmatrix} = \begin{bmatrix} D_{11} & \frac{|u_{tbond}|}{u_{tbond}} D_{12} \\ 0 & D_{22} \end{bmatrix} \begin{bmatrix} u_{nbond} \\ u_{tbond} \end{bmatrix} \quad (3)$$

where D_{12} normally is negative, meaning that slip in either direction will cause negative t_n , i.e. compressive forces directed outwards in the concrete. The yield surface is defined by two yield functions, one describing the friction F_1 , assuming that the adhesion is negligible. The other yield function, F_2 , describes the upper limit at a pull-out failure. It is determined from the stress in the inclined compressive struts that results from the bond action.

$$F_1 = |t_t| + \mu t_n = 0 \quad (4)$$

$$F_2 = t_t^2 + t_n^2 + c \cdot t_n = 0 \quad (5)$$

The yield surface is shown in Figure 1. For plastic loading along the yield function describing the upper limit, F_2 , an associated flow rule is assumed. For the yield function describing the friction, F_1 , a non-associated flow rule is assumed, for which the plastic part of the deformations is

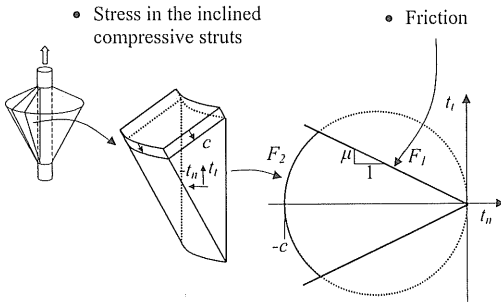


Figure 1. The yield surface of the bond model.

$$d\mathbf{u}^p = d\lambda \frac{\partial G}{\partial \mathbf{t}}, \quad G = \frac{|u_{tbond}|}{u_{tbond}} t_t + \eta t_n = 0. \quad (6)$$

For the hardening rule of the model, a hardening parameter κ is established.

$$d\kappa = \sqrt{du_{nbond}^p{}^2 + du_{tbond}^p{}^2} \quad (7)$$

The variables μ and c in the yield functions are assumed to be functions of κ . The model can also be used for cyclic loading.

3.2 Chosen input for the bond model

The input parameters were given as described in Lundgren (2000b). That is, the coefficient of friction, μ , was assumed to vary from 1.0 down to 0.4 during the hardening, and the parameter η was assumed to be constant for monotonic loading. The stress in the inclined compressive struts, i.e. the function $c(\kappa)$, was determined by the uniaxial compressive strength of the concrete, with a descending part. The stiffness D_{11} in equation (3) was assumed to depend on the deformation u_n . The other stiffnesses, i.e. D_{12} and D_{22} , were assumed to be constant.

4 CORROSION MODEL

4.1 Volume increase of the corrosion products

The volume increase of the corrosion products compared with the virgin steel was modelled in a corrosion layer. The volume of the rust relative to the uncorroded steel was given as input. Furthermore, the corrosion penetration x was given as a function of the time. The corrosion was then modelled by taking time steps.

The physical interpretations of the variables of the model are presented in Figure 2. By assuming that the volume of the rust (corresponding to the grey area in Figure 2) is v times the volume of the steel that has corroded (corresponding to the striped area in Figure 2), the distance a can be determined:

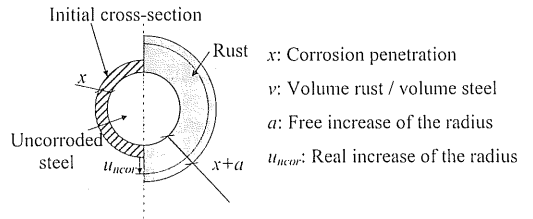


Figure 2. Physical interpretation of the variables in the corrosion model.

$$a = -r + \sqrt{r^2 + (v-1) \cdot (2rx - x^2)} \quad (8)$$

This is the free increase of the radius; i.e. if the radius is increased that much, the normal stresses will be zero. The real increase of the radius is u_{ncor} , corresponding to a strain in the rust:

$$\varepsilon_{cor} = \frac{u_{ncor} - a}{x + a} \quad (9)$$

From this strain in the rust, the normal stresses in the layer are determined; see the next section.

The volume of the rust relative to the uncorroded steel, v , is an important parameter in the model. This value depends on which corrosion product forms. Values from 2.2 to 6.4 are given in the literature. Most often, a value of 2.0 has been used in analyses of corrosion splitting; see Molina *et al.* (1993), Noghabai (1998), and Coronelli & Gambarova (2000). The latter value was also chosen here.

4.2 Mechanical behaviour of the rust

For the modelling of the corrosion layer, the mechanical behaviour of the corrosion products needs to be known. No information about this has been found in the literature. Molina *et al.* (1993) assume that the rust is elastic but state that “the properties of the rust should be replaced by others which are more realistic if a way can be found to obtain them”. Petre-Lazar & Gerard (2000) used a scratching test to investigate the mechanical properties of the corrosion products. They reached the conclusion that rust is a cohesionless assemblage of incompressible crystals.

To investigate the mechanical behaviour of rust, corrosion cracking tests found in the literature were studied. Ghandehari *et al.* (2000) have carried out pull-out tests on corroded reinforcement bars in concrete cylinders. Al-Sulaimani *et al.* (1990) and Cabrera & Ghoudoussi (1992) have carried out pull-out tests on corroded reinforcement bars concentrically placed in concrete blocks. To investigate the mechanical behaviour of rust, the first part of their experiments was studied, i.e. when the reinforcement corroded until the specimen was cracked. The corrosion penetration was measured by the weight loss method; from these measurements the corrosion penetration at cracking can be estimated. Axisymmetric finite element analyses of the test specimens were carried out. For the tests of Ghandehari *et al.* (2000) this corresponds to the geometry of the test specimen, and for the others it was accepted as a reasonable approximation. Only the concrete was then modelled, and a normal stress was applied at the hole in the centre of the cylinder. The concrete was modelled with a constitutive model based on

non-linear fracture mechanics, and four radial cracks were assumed. For more details of how the concrete was modelled, see the section 5.1.

Andrade *et al.* (1993) carried out corrosion cracking tests with reinforcement bars eccentrically placed in concrete blocks. Due to this placement, an axisymmetric approximation was not possible. Instead, two-dimensional models assuming plane strain were used. The normal stress was applied in the hole with deformation control.

Since the Young’s modulus is much larger for the steel than for the concrete, it can be assumed that the deformation of the reinforcement bar is negligible. The stiffness in the normal direction of the bond layer, D_{II} , is chosen large enough that the deformation of the bond layer is also negligible. Thereby, it can be concluded that the deformation at the hole approximately equals the deformation in the corrosion layer, u_{ncor} .

By combining the u_{ncor} obtained when cracking occurred in the analyses with the corrosion penetration at cracking from the experiments, a value of the strain in the rust could be calculated, using equations (8) and (9). The chosen value of 2.0 for the volume of the rust relative to the uncorroded steel was then used. This strain in the rust corresponds with the applied normal stress when cracking occurred in the analyses. The results are summarised in Figure 3, where the normal stress versus the strain in the rust is plotted. Although it must be noted that parameters known to have an influence on cracking – such as the applied current – varied for the tests analysed, this can give some information about the mechanical behaviour of the rust. The results indicate that the rust does not have a linear elastic behaviour. Instead, it was assumed that the rust behaves like a granular material; i.e. its stiffness increases with the stress level. This also corresponds

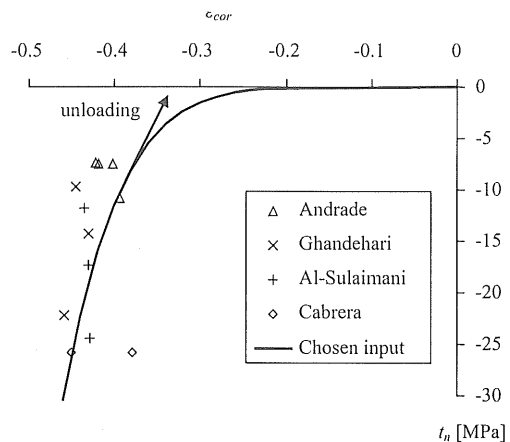


Figure 3. Normal stress versus strain in the rust evaluated from a combination of experimental results and analyses, together with the chosen input.

to the findings of Petre-Lazar & Gerard (2000) that rust is a cohesionless assemblage of incompressible crystals. It was assumed that the mechanical behaviour of the rust at loading could be described with the equation:

$$t_n = K_{cor} \cdot \varepsilon_{cor}^p \quad (10)$$

The parameters K_{cor} and p were chosen to give reasonable agreement with the results from the analyses of the tests; see Figure 3, where the curve for the chosen values of $K_{cor} = 7.0$ GPa and $p = 7.0$ is plotted together with the analysis results. Further, it was assumed that the rust was unloaded with the stiffness achieved, as indicated in Figure 3.

5 COMPARISON WITH TESTS

5.1 Finite element analyses

Tests of various kinds have been analysed with finite element models. In all analyses, the concrete was modelled with a constitutive model based on non-linear fracture mechanics. In analyses using the smeared crack concept, a rotating crack model based on total strain was used; see TNO (1998). For the axisymmetric models, four discrete radial cracks were assumed.

From the various measured compressive strengths, an equivalent compressive cylinder strength, f_{cc} , was evaluated. Other necessary material data for the concrete were estimated according to the expressions in CEB (1993) from f_{cc} . The constitutive behaviour of the reinforcement steel was modelled by the Von Mises yield criterion with associated flow and isotropic hardening. The elastic modulus of the reinforcement was assumed to be 200 GPa when it had not been measured.

5.2 Pull-out tests with uncorroded reinforcement

Pull-out tests of various kinds with uncorroded reinforcement have been analysed with finite element models. The tests have been selected to show various types of failure: pull-out failure, splitting failure, pull-out failure after yielding of the reinforcement, and rupture of the reinforcement bar. In all tests, the reinforcement is of type K500 ϕ 16, and the concrete is of normal strength (the compressive cylinder strength varies from 25 to 35 MPa).

5.2.1 Pull-out failure

In tests carried out by the author, see Lundgren (2000a), reinforcement bars were pulled out of concrete cylinders surrounded by steel tubes. The steel tubes had a diameter of 70 mm, a height of 100 mm, and a thickness of 1.0 mm. The embedment length of the reinforcement bars was 50 mm. The tangential strains in the steel tubes were measured

at three heights, together with the applied load and slip. Five tests were carried out, three in one direction and two in the other. These tests were used to calibrate the bond model. Results from the analyses, together with the finite element mesh used, are shown in Figure 4. Due to the confinement of the steel tube, pull-out failure was obtained, both in the tests and in the analyses.

Pull-out tests carried out by Magnusson (2000) and Balázs & Koch (1995) have also been analysed. Magnusson had concrete cylinders with a diameter of 300 mm and an embedment length of 40 mm; Balázs and Koch had concrete specimens with a quadratic cross-section 160·160 mm and an embedment length of 80 mm. In both cases, the concrete specimens were large enough to prevent splitting failure; thus, pull-out failures were obtained. Results from the analyses are compared with experiments in Figure 5. As can be seen, a reasonably good agreement was obtained.

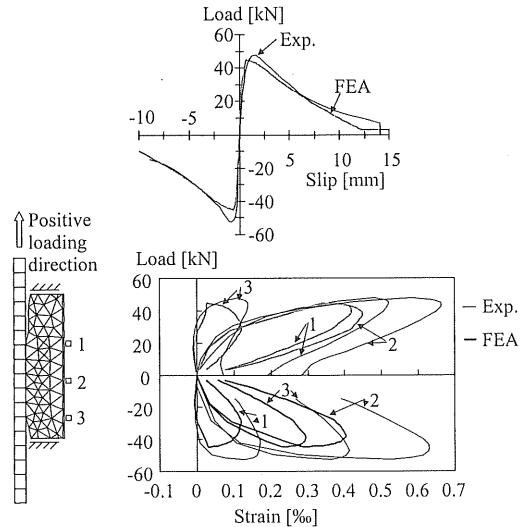


Figure 4. Comparison between test results and results from the analyses of the steel-encased pull-out tests.

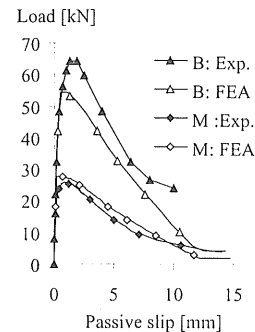


Figure 5. Load versus slip in pull-out-tests with short embedment length. The experimental results are from B: Balázs & Koch (1995) and M: Magnusson (2000).

5.2.2 Splitting failure

Magnusson (2000) has also carried out pull-out tests on eccentrically reinforced specimens with varying stirrup configurations. The different stirrup configurations (without stirrups, with two and with four stirrups along the embedment length) led to splitting failures at various levels. In the test specimen with four stirrups, the stirrups gave enough confinement to obtain a ductile failure after splitting. In the analyses of these experiments, the stirrups were modelled as embedded reinforcement, meaning that complete interaction between the stirrups and the concrete was assumed.

The results from the analyses are shown in Figure 6. It can be noted that even with the same embedment length, and when exactly the same input parameters were given for the interface, different load-slip curves were obtained depending on the modelled structure, in this case the number of stirrups. Comparing with the measured response, the agreement is good, especially when considering the large scatter that is always obtained in pull-out tests.

5.2.3 Yielding of the reinforcement

Magnusson (2000) has also carried out pull-out tests where the reinforcement had an embedment

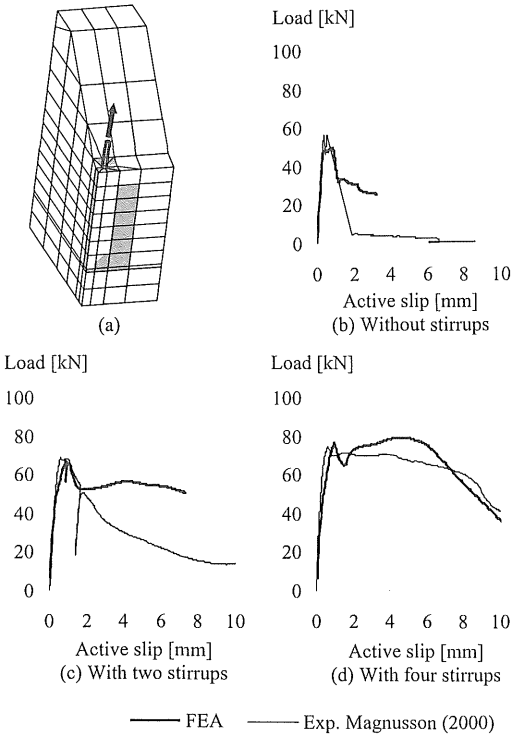


Figure 6. (a) Mesh used in analyses of eccentrically reinforced pull-out-tests; grey marked elements indicate cracked elements in the analysis without stirrups. (b), (c), and (d) Load versus slip for the eccentrically reinforced pull-out-tests.

length long enough to give yielding of the reinforcement. Two of these tests were analysed, where the reinforcement was centrally placed in a concrete specimen of dimensions 400·400 mm. In one of the experiments, with an embedment length of 220 mm, a pull-out failure after yielding of the reinforcement was obtained; and in the other one, with an embedment length of 360 mm, rupture of the reinforcement bar occurred. As can be seen in Figure 7 (when there is pull-out failure, there is a rather long descending branch, but when there is rupture of the reinforcement bar, the load falls straight down to zero), the same results were obtained in the analyses. In Figure 8, the bond-slip resulting from the analyses at various levels along the bar is shown. It can be

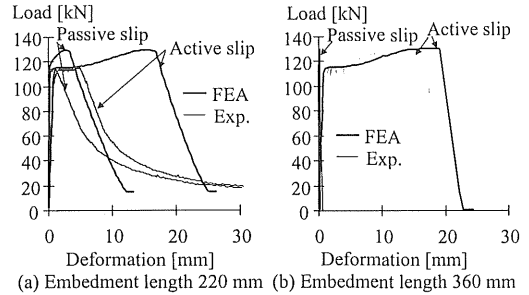


Figure 7. Load versus slip in pull-out-tests with long embedment length. Experimental results from Magnusson (2000).

seen that the bond stress decreased drastically when the reinforcement reached the yield plateau. This is because the normal stress decreased when the radius of the reinforcement bar decreased. When the reinforcement began to harden again, a small bond capacity was obtained. This was possible since the decrease of the radius of the reinforcement was lower when the reinforcement hardened, and thus, normal stresses could be built up again.

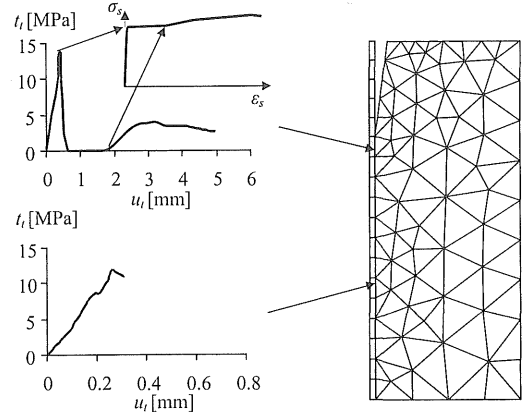


Figure 8. Bond stress versus slip at various integration points along the bar in pull-out-tests with embedment length 360 mm. The reinforcement elements that are marked grey reached yielding.

5.3 Corrosion cracking tests

Andrade *et al.* (1993) have carried out corrosion cracking tests. These were analysed with three-dimensional models, using the presented corrosion and bond model in interface elements between the reinforcement and the concrete. In the tests, the specimens were 15 cm·15 cm·38 cm. Here, slices of them were analysed, assuming fixed boundaries in the third direction, corresponding to a plane strain assumption. It was chosen to model the cracks with discrete crack elements. One of the finite element models is shown in Figure 9a. In Figure 9b, c, and d, comparisons between measured crack widths and crack widths obtained in the analyses are shown. As can be seen, the crack openings in the analyses are somewhat too small. One reason for this might be that the corrosion penetration was obtained in the tests by the use of Faraday's law. Later tests by Alonso *et al.* (1998), where they measured the corrosion penetration also by the weight loss method, indicated that the corrosion penetration was underestimated by Faraday's law. On this basis, larger corrosion penetrations should have been applied in the analyses, leading to improved agreement.

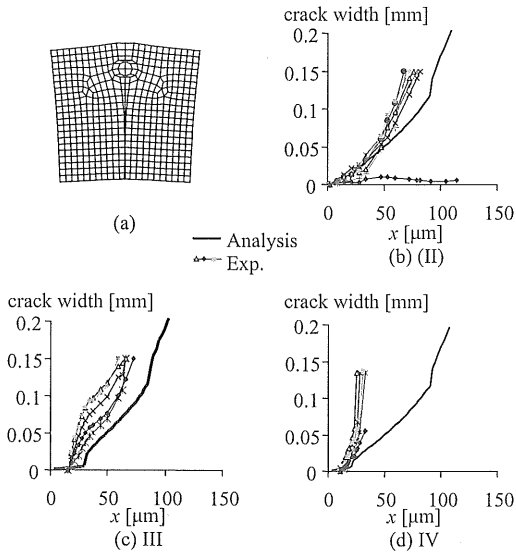


Figure 9. (a) Deformed mesh in analysis of test II using the bond and corrosion models in the interface elements between the steel and the concrete. (b), (c) and (d) Comparisons between crack widths, measured and obtained in the analyses, versus the corrosion penetration. Experimental results from Andrade *et al.* (1993).

5.4 Pull-out tests with corroded reinforcement

The pull-out tests on corroded reinforcement bars in concrete cylinders carried out by Ghandehari

et al. (2000) have been analysed. They used four different geometries: with cylinder diameters of 100 and 150 mm, and with rebar diameters of 9.5 and 20 mm. These were labelled CsRs, CsRl, CIRs, and CIRl, where C stands for the concrete cylinder diameter, R for the rebar diameter, and s and l for small and large. The specimens were 50-mm slices, and were subjected to accelerated constant current corrosion for four weeks. The rebar in each slice was tested in pull-out to investigate the bond strength after 0, 1, 2, 3, and 4 weeks of corrosion. The corrosion penetration was evaluated both by using Faraday's law from the applied current, and by measuring the weight loss for the reinforcement in each slice. Here, the measured corrosion penetration (evaluated from the weight loss) was used as input.

Axisymmetric finite element analyses were carried out, with the specially developed interface elements describing the corrosion of the reinforcement bar and the bond mechanism. In the analyses, the corrosion was first applied as time steps. When the corrosion penetration measured in the experiments was reached, the reinforcement bar was pulled out of the concrete cylinder. In the analyses, only the failure of CIRs was a pull-out failure, while all the other three were splitting failures, both for the uncorroded

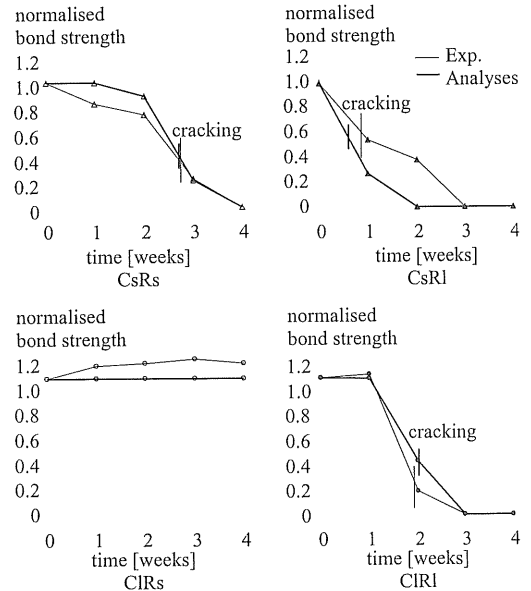
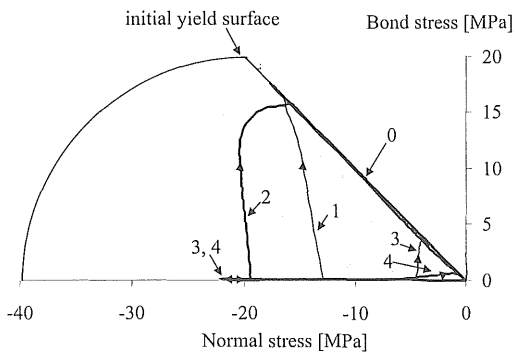
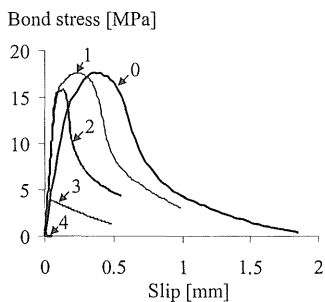


Figure 10. Comparisons between normalised bond strength, measured and obtained in the analyses versus the time. Experimental results from Ghandehari *et al.* (2000).

pull-out and for the pull-out tests after corrosion. It is not described by Ghandehari *et al.* (2000) which type of failure occurred in the experiments. However, since the capacity of specimen CIRs was



(a)



(b)

Figure 11. Results from the analyses of test specimen CsRs.

slightly increased when the reinforcement had corroded, while for the others it was decreased, pull-out failure of specimen CIRs and splitting failure of the others was most likely the case also for the tests.

From each of the pull-out analyses, the maximum load was compared with the maximum load obtained when the reinforcement was uncorroded. In Figure 10, a comparison between the measured bond strengths and those from the analyses is shown. The corrosion penetration when cracking penetrated the cover is also marked. Only one minor difference between the experimental and analytical results can be noted: that the maximum capacity is not increased for small corrosion penetration in the analyses of the CIRs specimen, as it was in the tests. Else, the agreement between the tests and the analyses is good.

In Figure 11, some results from the analyses of test specimen CsRs are shown. The analyses are numbered according to how many weeks of corrosion the applied corrosion level corresponds to, before the reinforcement bar was pulled out of the concrete. The bond stress is plotted versus the normal stress in Figure 11a. In analysis CsRs0, no corrosion was applied. Therefore, both bond stresses and normal stresses were applied already from the beginning. In the other analyses, the applied corrosion led to an increase in only the normal stress, while the

bond stresses were zero before the pull-out force was applied. Naturally, increasing corrosion level led to increasing applied normal stresses. In the analyses of the tests CsRs3 and CsRs4 (three respective for weeks of corrosion), the specimens were cracked due to the corrosion only. While the specimen still had some capacity left to carry normal stresses, a small bond capacity could be obtained, even though it is hardly visible in the graph for CsRs4 (the bond capacity was only 0.6 MPa). In Figure 11b, the bond stress versus the slip from the analyses with varying corrosion level applied are compared. As can be seen, both the bond capacity and the slip when the maximum is obtained are decreased for increasing corrosion level.

6 CONCLUSIONS

A model describing bond between deformed reinforcement bars and concrete was developed. Since the model takes the three-dimensional splitting effect into account, the same input parameters will result in different load-slip curves depending on whether the reinforcement starts yielding, and on the geometry and strength of the surrounding structure. Steel-encased pull-out tests, where the tangential strain in the steel tubes had been measured, were used to calibrate the model.

The mechanical behaviour of rust was studied by a combination of analyses with test results found in the literature. This led to the assumption that rust behaves like a granular material, i.e. its stiffness increases with the stress level. This mechanical behaviour, and the volume increase of the corrosive products compared with the virgin steel, were modelled in a corrosion layer. The corrosion layer was combined with the developed model of the bond mechanism. By combining these models, the effect of corrosion on the bond strength can be analysed for diverse structures, and the effect of varying cover, stirrups, outer pressure, etc., can be investigated.

Comparing with the measured response from different experiments, the agreement is rather good. The failure mode is the same as in experiments in all of the analyses carried out. The decrease of bond due to splitting of the concrete, yielding of the reinforcement, or corrosion of the reinforcement, could be predicted. Comparisons between analyses of corrosion cracking tests and test results found in literature indicate reasonable agreement. Furthermore, analyses of pull-out tests with corroded reinforcement bars show that this way of modelling can predict the decrease of bond when splitting of the concrete occurs, due to the combined action of corrosion and the bond mechanism.

Here, tests with accelerated corrosion have been analysed. In order to investigate the effect of corro-

sion in real structures, long-term effects such as creep and shrinkage of the concrete must probably be included in the analyses, as pointed out by Noghabai (1998). Furthermore, the corrosion attack penetration has been given as a function of the time as input in the analyses. In future research, it would be most interesting to include this time-dependence in the analysis so that various environments, concrete cover and cracking could influence the corrosion rate and volume increase. Thereby, it would be possible to investigate a structure's lifetime and to determine the effect of various environments on, for example, the structure's deformations and load-bearing capacity.

REFERENCES

- Alonso, C., Andrade, C., Rodriguez J., & Diez, J. M. 1998. Factors controlling cracking of concrete affected by reinforcement corrosion. *Materials and Structures* 31: 435-441.
- Al-Sulaimani G. J., Kaleemullah M., Basunbul I. A., & Rasheeduzzafar 1990. Influence of corrosion and cracking on bond behaviour and strength of reinforced concrete members. *ACI Structural Journal* 87 (2): 220-231.
- Andrade, C., Alonso, C., & Molina, F. J. 1993. Cover cracking as a function of bar corrosion: Part 1 – Experimental test. *Materials and Structures* 26: 453-464.
- Balázs G. & Koch R. 1995. Bond characteristics under reversed cyclic loading. *Otto Graf Journal* 6: 47-62.
- CEB 1993. *CEB-FIP Model Code 1990*. CEB Bulletin d'Information No. 213/214. Lausanne: CEB.
- Cabrera J. G. & Ghoddoussi P. 1992. The effect of reinforcement corrosion on the strength of the steel/concrete "bond". In *Bond in Concrete, Proceedings of an International Conference, Riga 1992*. Riga: CEB.
- Coronelli D. & Gambarova P. G. 2000. A mechanical model for bond strength of corroded reinforcement in concrete. In *Proceedings EM2000, Fourteenth Engineering Mechanics Conference, Austin, Texas, USA, May 2000*. Austin: ASCE.
- Ghandehari M., Zulli M. & Shah S. P. 2000. Influence of corrosion on bond degradation in reinforced concrete. In *Proceedings EM2000, Fourteenth Engineering Mechanics Conference, Austin, Texas, USA, May 2000*. Austin: ASCE.
- Lundgren, K. 1999. *Three-dimensional modelling of bond in reinforced concrete: theoretical model, experiments and applications, Publication 99:1*. Göteborg: Chalmers University of Technology, Division of Concrete Structures.
- Lundgren, K. 2000a. Pull-out tests of steel-encased specimens subjected to reversed cyclic loading. *Materials and Structures* 33 (August-September): 450-456.
- Lundgren K. 2000b. *Bond between corroded reinforcement and concrete, Report 00:3*. Göteborg: Chalmers University of Technology, Department of Structural Engineering, Concrete Structures.
- Lundgren, K. & Gylltoft, K. 2000. A model for the bond between concrete and reinforcement. *Magazine of Concrete Research* 52 (1): 53-63.
- Magnusson J. 2000. *Bond and Anchorage of Ribbed Bars in High-Strength Concrete, Publication 00:1*. Göteborg: Chalmers University of Technology, Division of Concrete Structures.
- Molina, F. J., Alonso, C., & Andrade, C. 1993. Cover cracking as a function of rebar corrosion: Part 2 – Numerical model. *Materials and Structures* 26: 532-548.
- Noghabai, K. 1998. *Effect of tension softening on the performance of concrete structures, Ph. D. Tesis 1998:21*. Luleå: Luleå University of Technology, Division of Structural Engineering.
- Petre-Lazar, I. & Gerard, B. 2000. Mechanical behaviour of corrosion products formed at the steel – concrete interface. Testing and modelling. In *Proceedings EM2000, Fourteenth Engineering Mechanics Conference, Austin, Texas, USA, May 2000*. Austin: ASCE.
- TNO Building and Construction Research 1998. *DIANA Finite Element Analysis, User s Manual release 7*. Hague: TNO Building and Construction Research.